HHS Public Access

Author manuscript

Bone. Author manuscript; available in PMC 2019 August 01.

Published in final edited form as:

Bone. 2016 November ; 92: 180–188. doi:10.1016/j.bone.2016.09.001.

Sost, independent of the non-coding enhancer ECR5, is required for bone mechanoadaptation

Alexander G. Robling[1,2], **Kyung Shin Kang**[1], **Whitney A. Bullock**[1], **William H. Foster**[3], **Deepa Murugesh**[4], **Gabriela G. Loots**[4,5], **Damian C. Genetos**[5,*]

[1]Department of Anatomy & Cell Biology, Indiana University School of Medicine, Indianapolis, IN 46202, USA.

[2]Department of Biomedical Engineering, Indiana University/Purdue University at Indianapolis, Indianapolis, IN 46202, USA.

[3]Department of Anatomy, Physiology and Cell Biology, University of California Davis, Davis, CA, USA.

[4]Biology and Biotechnology Division, Lawrence Livermore National Laboratory, Livermore, CA 94550, USA.

[5]Molecular and Cell Biology Unit, School of Natural Sciences, University of California at Merced, Merced, CA, USA.

Abstract

Sclerostin (*Sost*) is a negative regulator of bone formation that acts upon the Wnt signaling pathway. *Sost* is mechanically regulated at both mRNA and protein level such that loading represses and unloading enhances *Sost* expression, in osteocytes and in circulation. The non-coding evolutionarily conserved enhancer *ECR5* has been previously reported as a transcriptional regulatory element required for modulating *Sost* expression in osteocytes. Here we explored the mechanisms by which *ECR5*, or several other putative transcriptional enhancers regulate *Sost* expression, in response to mechanical stimulation. We found that *in vivo* ulna loading is equally osteoanabolic in wildtype and $Sost^{-/-}$ mice, although *Sost* is required for proper distribution of load-induced bone formation to regions of high strain. Using Luciferase reporters carrying the *ECR5* non-coding enhancer and heterologous or homologous h*SOST* promoters, we found that *ECR5* is mechanosensitive *in vitro* and that ECR5-driven Luciferase activity decreases in osteoblasts exposed to oscillatory fluid flow. Yet, $ECR5^{-/-}$ mice showed similar magnitude of load-induced bone formation and similar periosteal distribution of bone formation to high-strain regions compared to wildtype mice. Further, we found that in contrast to $Sost^{-/-}$ mice, which are resistant to disuse-induced bone loss, $ECR5^{-/-}$ mice lose bone upon unloading to a degree similar to wildtype control mice. *ECR5* deletion did not abrogate positive effects of unloading on *Sost*, suggesting that additional transcriptional regulators and regulatory elements contribute to load-induced regulation of *Sost*.

*Authors for correspondence (dgenetos@ucdavis.edu).

Keywords

Sost; Sclerostin; mechanotransduction; ECR5; enhancer; skeleton; disuse

INTRODUCTION

Mechanical signals are an important factor in shaping the skeleton during development, growth and maintenance. Reduced mechanical stress or unloading, leads to significant bone loss[1], while increased mechanical stress or loading, causes an increase in bone mass[2]. It was originally hypothesized that the osteocyte is the primary cell type in bone tissue that senses strain[3], Mechanically perturbed osteocytes produce secreted molecules that ultimately modulate the activity of osteoblasts and osteoclasts on the bone surfaces. One of the key mechanosensitive osteocyte products is the Lrp5/6 antagonist sclerostin—the protein product of the *SOST* gene. *In vivo* loading and unloading experiments conducted in rodent models consistently yield changes in *Sost*/sclerostin levels in the affected limb bones, wherein sclerostin is significantly reduced in loaded limbs and significantly increased in limbs subjected to disuse [4–6]. The regulation of sclerostin during mechanotransduction has important functional consequences. For example, mice harboring a transgene that prevents *SOST* downregulation during mechanical loading (*Dmp1*-h*SOST*) fail to exhibit an osteogenic response to *in vivo* mechanical stimulation[7]. Conversely, preventing the increase in *Sost* expression that normally accompanies disuse, either by deleting the gene[8] or by inactivating the protein *via* antibody-mediated neutralization [5], protects mice from disuse-induced bone loss.

As osteocyte-derived *Sost* is a critical permissive factor for bone loss under disuse conditions, there is considerable interest in understanding the mechanisms that control *Sost* transcription, particularly since modulation of *Sost* levels is a critical process in fine tuning bone tissue's anabolic/catabolic responses to loading or disuse. Despite the interest in *Sost* function and the effect of sclerostin inhibition as an osteoanabolic agent, there are relatively few studies that identify mechanistically how *Sost* is transcriptionally regulated. However, clues to mechanisms of Sost regulation can be found in the "natural experiment" of the rare skeletal disorder van Buchem's (VB) disease. VB patients exhibit very high bone mass and a near complete lack of SOST expression, yet the *SOST* coding sequence, intron, promoter, and UTR sequences are not mutated, *i.e.*, are genotypically normal; instead, the suppression of *SOST* in these patients is due to a 52kb deletion in the intergenic region—35kb downstream of *SOST*—between *SOST* and *MEOX1*[9,10]. We recently identified a small 255bp fragment within the 52kb VB region, designated as *ECR5,* that is essential for *Sost* expression in osteocytes *in vitro* [11]. Deletion of *ECR5* from the mouse genome resulted in a significant decrease in *Sost* transcription and a high bone mass phenotype[12]. The significance of the ECR5 sequence in Sost transcription was further highlighted in *in vitro* experiments, where the induction of Sost expression by transforming growth factor-β (Tgf-β) was dependent upon the ECR5 enhancer rather than the proximal *Sost* promoter[13].

If *ECR5* is necessary and sufficient for the transcriptional activation of *Sost* in osteocytes, and if ECR5 activity is sensitive to mechanical stimulation, then $ECR5^{-/-}$ and $Sost^{-/-}$ mice

should respond similarly to loading and unloading. Conversely, the milder HBM phenotype observed in *ECR5*$^{-/-}$ mice, compared to *Sost*$^{-/-}$ mice, could implicate additional or alternative mechanisms that govern the mechanical regulation of *Sost* expression in bone. To evaluate these possibilities, we examined the requirement of *Sost* and *ECR5* for *in vivo* load-induced bone formation and for *in vivo* disuse-induced bone loss. We further conducted *in vitro* experiments designed to determine whether the *ECR5* sequence is active during mechanical stimulation. Whereas Sost$^{-/-}$ mice were protected from the bone-wasting effects of mechanical disuse, *ECR5*$^{-/-}$ mice were not protected from disuse-induced bone loss. Despite exhibiting lower overall *Sost* expression, *ECR5*$^{-/-}$ mice were able to upregulate *Sost* in response to tail suspension. Ulnar loading was equally osteogenic in wildtype, *Sost*$^{-/-}$, and *ECR5*$^{-/-}$ mice, but only *Sost*$^{-/-}$ mice exhibited a perturbed distribution of new load-induced bone formation that exhibited compromised preference for high-strain regions of the cortex. Further functional dissection of *Sost*'s genomic domains is required to identify additional transcriptional regulatory elements that modulate *Sost* expression in response to mechanical stimulation.

MATERIALS AND METHODS

Mice

This study was carried out in strict accordance with the recommendations in the Guide for the Care and Use of Laboratory Animals of the National Institutes of Health. The animal protocols were approved by the Indiana University Institutional Animal Care and Use Committee (IACUC). Generation of mice with the high-bone-mass-causing *Sost* mutation have been described previously[14]. Briefly, *Sost*$^{+/-}$ mice were engineered by replacing approximately 90% of the *Sost* coding sequence and all of the single intron, with a neomycin-resistance cassette, *via* homologous recombination. Generation of mice with the high bone mass-causing *ECR5* deletion mutation have been described previously [12]. Briefly, a 338-bp *ECR5* region was replaced with a floxed neomycin cassette using Velocigene and homologous recombination. *ECR5*$^{+/-}$ mice crosses were used to generate experimental *ECR5*$^{-/-}$ mice. The genetic background of the *Sost* mutant mice was a uniform mixture of 129S1/SvIMJ and C57Bl/6J. The genetic background of the *ECR5* mutant mice was C57Bl/6J. Sixteen-week old mice were used for the disuse experiments. Male mice were used for the tail suspension studies (see below) and female mice were used for the Botox and ulnar loading studies. In each experiment, sample sizes for each genotype treatment included 8–10 mice per group, except for the gene expression studies, which included n=6/group.

Ex vivo *strain gauging,* in vivo *ulnar loading, and fluorochrome labeling*

When the animals reached 16 wk of age, five mice from each strain (*Sost*$^{+/+}$, *Sost*$^{-/-}$, *ECR5*$^{+/+}$, *ECR5*$^{-/-}$) were chosen at random, anesthetized, and sacrificed by cervical dislocation. Immediately after death, the right forearm was minimally dissected to expose the medial surface of the midshaft ulna. A single element strain gauge (EA-06–015DJ-120; Measurements Group, Raleigh, NC, USA) was bonded to the exposed medial ulnar surface at midshaft. Once fitted with a strain gauge, the forearm was loaded in cyclic axial compression using an electromagnetic actuator with feedback control. Using a 2-Hz

haversine waveform, the forearms were loaded at 1.17, 1.40, 1.62, 1.85, and 2.07 N, during which voltage output from the strain gauge was recorded on a digital oscilloscope. Voltage measurements were converted to strain using a calibration factor derived from measured and calculated (using beam theory) strains collected from an aluminum cantilever. Strain per unit force ($Sost^{+/+}$ = 920 με/N; $Sost^{-/-}$ = 525με/N; $ECR5^{+/+}$ =955 με/N; $ECR5^{-/-}$ = 915 με/N) was used to adjust peak loads to deliver equal strain stimulus among the three load groups.

At 16 weeks of age, 30 female mice from each of the genotypes ($Sost^{+/+}$, $Sost^{-/-}$, $ECR5^{+/+}$, $ECR5^{-/-}$) began the ulnar loading regimen. We chose to conduct the loading experiments at 16 weeks of age because at this timepoint, the mice have reached skeletal maturity and the effects of loading, rather than growth, on ulnar bone formation rates are easily discernible. A haversine waveform was used to apply load (1800, 2300, or 2800 με) to the forelimb using a customized electromagnetic actuator at 2 Hz, for 180 cycles/day. Each mouse was loaded 3dy/wk for 2 wks. Calcein (12 mg/kg IP) and alizarin complexone (20 mg/kg IP) were injected 5 and 14 days, respectively, after the last first bout. Mice were sacrificed 8 days after the alizarin injection. At sacrifice, the left (unloaded) and right (loaded) ulnae were dissected, cleaned and fixed in 10% NBF for 2 days followed by storage in 70% ethanol at 4°C.

Quantitative histomorphometry

The fixed ulnae were dehydrated in graded ethanols, cleared in xylene, and embedded in methylmethacrylate. Thick sections were collected at 1 to 1.5 mm distal to the midshaft using a diamond-embedded wafering saw. Sections were ground and polished to ~30 μm, mounted and coverslipped, then digitally imaged on a fluorescent microscope. Periosteal bone formation parameters were calculated by measuring the extent of unlabeled perimeter, single-labeled perimeter (sL.Pm), double-labeled perimeter (dL.Pm), and the area between the double labeling with Image-Pro software (MediaCybernetics Inc., Gaithersburg, MD). Derived histomorphometric parameters were calculated using standard procedure, which are mineralizing surface over bone surface (MS/BS = ((0.5 × sL.Pm + dL.Pm) / total perimeter × 100) (%)), mineral apposition rate (MAR = double labeled area / dL.Pm / 8 days) (μm/day)), and bone formation rate (BFR/BS = MAR × MS / BS × 3.65) ($\mu m^3/\mu m^2$/year)). Relative load-induced bone formation parameters were calculated by subtracting the control arm value from the loaded arm value for each mouse. For sectoral analysis of regional bone formation along the periosteal surface, an “H” shaped mask was created in Image-Pro and superimposed onto each rotated ulnar section image (see Figure 2). The mask was generated by positioning a line extending in the dorso-ventral direction at a point 40% of the distance from the medial surface to the lateral surface. A second line was positioned extending in the dorso-ventral direction at a point 80% of the distance from the medial surface to the lateral surface. A third line was positioned medio-lateral direction that was perpendicular to the two dorso-ventral lines and also passed throught the center of mass of the section. Dorso-ventral line placement was chosen based on the calculated shift in neutral axis that occurs with bending and superimposed axial compression in the mouse ulna [15]. Labeling parameters were remeasured within the boundary of each of the four sectors, then summarized across opposite cortices (caudal with cranial, medial with lateral).

Plasmid transfection and oscillatory fluid flow in vitro

UMR106.1 rat mature osteoblasts were seeded onto 75×38×1.0mm glass slides (400,000 cells/slide). The next day, cells were co-transfected with 500ng *Renilla* luciferase under control of the thymidine kinase promoter (pRL-TK-Luc; Promega) and 1μg of pGL3-based (Promega) *Firefly* luciferase reporter plasmids with X-TremeGENE HD (Roche) in Opti-MEM (Invitrogen). The pGL3-based reporter plasmids contain the human *SOST* promoter only (h*SOST*-Luc) or three copies of the ECR5 enhancer upstream of the human *SOST* promoter (3xECR5-h*SOST*-Luc) [11,13]. Twenty-four hours after transfection, slides were placed into oscillatory fluid flow chambers in flow media (MEM supplemented with 2% fetal bovine serum, 1% penicillin-streptomycin, 20 mM HEPES, pH 7.2) and were subjected to a oscillatory fluid flow with a peak shear stress of ± 20 dynes/cm^2, 1 Hz for 6 hours at 37°C, as described previously [16]. The flow rate was monitored with an ultrasonic flow meter (Transonic Systems, Ithaca, NY) during all experiments. Immediately after cessation of oscillatory fluid flow, cells were scraped from the slide in Passive Lysis Buffer, after which luciferase activity in recovered lysates was determined using the Dual-Luciferase Reporter Assay System (Promega) and a Turner Designs Model 20/20 Luminometer. Within each sample, firefly luciferase activity was normalized to pRL-TK to compensate for potential variations in transfection efficiency or cell number.

Dual energy x-ray absorptiometry (DEXA)

In some of the experiments, whole-body in vivo DEXA scans were collected to assess changes in bone mass as a result of the mechanical intervention. Scans were collected two days prior to the start of the experiment and again at sacrifice. Mice were anesthetized with isofluorane (2% @ 1.5 liters/min) during the procedure. Lower limb bone mineral content (BMC) was measured by adjusting the region of interest box to accommodate the lower limb distal to the acetabulum.

Micro-computed tomography (μCT)

μCT measurements of the midshaft and distal femur were collected in order to assess differences in cortical and trabecular architecture/mass changes as a result of the mechanical intervention. The right femur was extracted at sacrifice to use in μCT analyses (Scanco μCT 35) as described previously [17]. The bones were placed in 10% NBF for 2 days and then stored in 70% ethanol at 4°C. A 2.6-mm span of the distal femoral metaphysis was scanned on a high resolution μCT (μCT 35; Scanco Medical AG) at 13-μm resolution using 50-kV peak tube potential and 151-ms integration time to measure trabecular three-dimensional morphometric properties as previously described. Bone volume fraction (BV/TV) and trabecular thickness were calculated using standard algorithms.

Peripheral quantitative computed tomography (pQCT)

In some experiments pQCT scans through right proximal tibia were collected to assess changes in bone mass as a result of the mechanical intervention. pQCT scans were collected two days prior to the start of the experiment and again at sacrifice. Mice were anesthetized with isofluorane (2% @ 1.5 liters/min) during the procedure. The lower limb was secured to a platform that was centered in the gantry of a Norland Stratec XCT Research SA+ pQCT

(Stratec Electronics, Pforzheim, Germany). A single cross-sectional level was scanned approximately 4 mm distal to the proximal growth plate using a slice thickness 0.26 mm at a collimation of 4×10^5 counts/sec and at a voxel size of 0.07 mm. For each slice, x-ray source was rotated through 180° of projection for 1 block. The slice through the proximal tibia includes the cortical shell and secondary spongiosa. For each slice, total volumetric bone mineral content was measured from the pQCT images. Density thresholds of 500 and 900 mg/cm^3 were used to identify mineralized bone.

Hindlimb Suspension

Hindlimb-suspended mice were individually housed in shoebox cages and a tail harness was used to suspend the experimental mice as previously described[17]. Control mice were permitted unencumbered normal movement in their cages. Mice in the bone loss studies were suspended for a total of 24 days prior to sacrifice. *ECR5* mice used for gene expression were suspended for 4 days.

Statistical analysis

For the tail suspension studies, pre-intervention and post-intervention DEXA or pQCT measurements were compared. A paired t-test was used to determine if a difference occurred between the initial and final measurements within a genotype/treatment group. The percent change of a measurement from initial to final time points for each animal was calculated and the means of these percent changes were compared using student's t-test within genotype. For non-serial comparisons, two-way ANOVAs were conducted, using mechanical stimulus and genotype as main effects, and interaction terms were tested for significance as part of the main ANOVA model. *Post-hoc* follow up tests were performed using Fisher's protected LSD tests. Statistical significance was taken at $p < 0.05$. Data are presented as mean ± standard error.

For *in vitro* experiments, each independent trial composed of samples in triplicate or quadruplicate, and trials were repeated a minimum of three independent times. Unless otherwise noted, Luciferase data were normalized to internal control pRL-TK, and then to vehicle control to account day-to-day transfection variability, and are presented as mean +/− SEM.

RESULTS

Enhanced mechanical stimulation is equally osteogenic in wildtype *and* Sost$^{-/-}$ *mice*

We have shown that *Sost* is tightly regulated by the mechanical loading environment[4], and that forced transgenic expression of *SOST* during loading prevents load-induced bone formation[7]. Because sclerostin reduction is a key step in load-induced bone formation, we investigated whether complete deletion of *Sost* would alter load-induced bone formation. 16-wk-old female wildtype and *Sost*$^{-/-}$ mice were subjected to ulnar loading at one of three strain magnitudes (1800, 2300, or 2800με). Periosteal bone formation occurred in each genotype in a strain-dependent manner (Figure 1A). Relative mineralizing surface (Figure 1B), apposition rates (Figure 1C), and bone formation rates (Figure 1D) were increased in a strain-dose responsive manner in both wildtype and *Sost*$^{-/-}$ mice. No mutation-related

differences in periosteal osteogenic response were noted for any of the parameters, using genotype as a main effect.

Sost *is required for proper localization of new bone to surfaces experiencing high strains*

While measuring the fluorochrome-labeled sections, we noticed that the periosteal regions that experience minimal change in strain during ulnar loading (*i.e.*, along the neutral axis) appeared more heavily labeled in *Sost*$^{-/-}$ mice compared to wildtype mice (Figure 2A). To assess this difference, we went back and re-measured the histological sections using a sectoral approach, and quantified the same bone formation parameters separately in the medial, lateral, caudal, and cranial sectors. Among wildtype mice, bone formation rates were significantly greater in the high strain sectors (medial and lateral cortices) compared to *Sost*$^{-/-}$ mice (Figure 2B). Further, wildtype mice exhibited significantly lower bone formation rates in the low strain sectors (caudal and cranial cortices) compared to *Sost*$^{-/-}$ mice (Figure 2C).

The ECR5 enhancer is mechanosensitive in vitro

Previously, we have demonstrated that short-term (two hours) of oscillatory fluid shear stress significantly suppresses *Sost* mRNA expression, which subsequently recovered to baseline (static controls) levels within four hours post-fluid flow[18], suggesting that mechanical loading and unloading transcriptionally regulate *Sost* expression. *In vivo*, mechanical loading decreases *Sost* mRNA and sclerostin protein expression in osteocytes[4], and reductions in *Sost* are required for load-induced periosteal bone formation [7]. Yet, these data fail to identify whether the *Sost* promoter or the distal enhancer *ECR5* are responsive to biophysical forces.

To determine whether the osteocyte enhancer *ECR5* is mechanosensitive, we transfected UMR106.1 cells with different ECR5/SOST reporter constructs, applied fluid flow (peak shear stress of 20 dynes/cm^2), and measured reporter activity. Exposure to fluid flow significantly increased Luciferase activity in cells transfected with SV40-Luc or h*SOST*-Luc compared to plasmid-matched static cells (Figure 3B). SV40-Luc and *SOST*-Luc constructs increased reporter activity by 43% and 79% over static controls, respectively. In contrast, cells transfected with plasmids containing ECR5, regardless of the choice of heterologous SV40 or *SOST* promoter, decreased Luciferase activity in response to fluid flow, compared to static cells (Figure 3B).

We examined the kinetics of fluid flow-mediated changes in reporter activity. One hour of fluid flow did not significantly influence Luciferase activity, regardless of the plasmid's regulatory sequence (Figure 3C). Instead, significant increases in Luciferase activity in *SOST* were observed after 3 or 6 hours of fluid flow only in cells whose plasmid contained ECR5. Altering the number of copies of ECR5 (0, 1[13], or 3) in cells exposed to fluid flow dose-dependently decreased Luciferase activity, such that each additional copy amplified the repression (Figure 3D; Pearson correlation r=−0.9951). These results demonstrated that *ECR5* element responds to mechanical load to down-regulate transgene expression.

Mechanical loading increases bone formation in ECR5$^{-/-}$ *mice*

ECR5 deficient mice (*ECR5*$^{-/-}$) have a high bone mass phenotype due to reduced *Sost* expression in osteocytes[12]. To determine whether *ECR5*$^{-/-}$ mice phenocopy Sost$^{-/-}$ mice regarding their response to mechanical loading, we subjected *ECR5*$^{-/-}$ and WT littermate mice to ulnar loading using a single, matched peak strain magnitude. Relative mineralizing surface, apposition rates, and bone formation rates were increased by loading in both *ECR5*$^{-/-}$ and wildtype control mice (Figure 4), but no significant genotype-related differences were found for those parameters (Figure 4B–4D). We conducted a sectoral analysis of bone formation rates as described earlier for *Sost*$^{-/-}$ mice, but no differences in high strain regions (medial and lateral cortices; Figure 4E) or low strain regions (cranial and caudal cortices; Figure 4F) were detected between genotypes. These data suggest that mechanical loading increases bone formation and localization to high strain regions independent of ECR5.

Sost *deficiency prevents bone loss caused by unloading*

We and others have reported that mechanical disuse increases *Sost* expression *in vitro* [6] and *in vivo*[4]. To evaluate whether changes in *Sost* expression that occur with disuse have functional consequences on bone mass, we measured the effects of tail suspension on hindlimb bone mass and structural properties in 16-wk-old male *Sost*$^{-/-}$ mice (Figure 5A). Wildtype tail-suspended mice lost ~20% of their initial proximal tibia bone mineral content (BMC), whereas the ground control wildtype littermates did not lose a significant amount of proximal tibia BMC over the 24 day study (*i.e.*, BMC change was not significantly different from zero). Conversely, the same comparison among *Sost*$^{-/-}$ mice revealed that tail suspended mice did not lose a significant amount of proximal tibia BMC (change was not significantly different from zero), but the ground control *Sost*$^{-/-}$ littermates gained a significant amount of BMC (Figure 5B), which resulted in a significant difference between ground control and tail suspended *Sost*$^{-/-}$ groups. In the distal femur, trabecular bone volume fraction (BV/TV) and trabecular thickness (Tb.Th) were significantly reduced by tail suspension in wildtype but not *Sost*$^{-/-}$ mice (Figures 5A, 5C, and 5D). Regardless of genotype or mechanical intervention, mice did not gain nor lose a significant amount of body weight during the course of these experiments (Figure 5E). Similar results were observed in wildtype or *Sost*$^{-/-}$ mice in which neuromuscular transmission was inhibited with Botox (Supplemental Figure 1).

ECR5 deficient mice are not protected from the bone-wasting effects of disuse

Because *Sost*$^{-/-}$ mice are protected from the bone-wasting effects of disuse (presumably because Sost cannot be upregulated during disuse), and considering that *Sost* expression is at least partially under the control of *ECR5*, we next asked whether deletion of *ECR5* is sufficient to prevent *Sost* upregulation during disuse, and ultimately, prevent disuse-induced bone wasting. *ECR5*$^{-/-}$ and *ECR5*$^{+/+}$ mice were tail suspended or housed in ground control conditions for 24 days (for skeletal microarchitecture) or 4 days (for gene expression). Wildtype mice lost ~7.5% of their proximal tibia BMC as a result of tail suspension, whereas *ECR5*$^{-/-}$ mice lost ~10% BMC (Figures 6A and 6B). Trabecular bone volume decreased in each genotype under disuse conditions; there was a modest, statistically

significant difference, in trabecular bone volume between wildtype and *ECR5*$^{-/-}$ mice under both control and suspended conditions, yet the relative decrease in trabecular BV/TV (Figure 6C) and trabecular thickness (Figure 6D) was the same regardless of genotype, suggesting that lack of *ECR5* renders a disuse bone loss phenotype similar to wildtype mice.

Having observed that *Sost* is required for disuse-induced bone loss and because *ECR5*$^{-/-}$ have a significant reduction in *Sost* expression [12], we sought whether *ECR5* deficiency affects disuse-dependent transcriptional upregulation of *Sost*. Wildtype or *ECR5*$^{-/-}$ mice were subjected to 4 days of tail suspension or ground control conditions, after which femoral or tibial cortical bone RNA was isolated, purified, and analyzed for *Sost* expression. *Sost* expression was significantly increased in both tail suspended wildtype and *ECR5*$^{-/-}$ mice (Figure 6E), suggesting that disuse-mediated upregulation of *Sost* transcription is independent of the *ECR5* osteocyte enhancer.

DISCUSSION

The skeleton adapts to the demands of its mechanical environment. Although this has been appreciated for centuries, how biophysical signals translates into an adaptive response remains an unresolved field that is currently under worthy of investigation. Osteocytes are the most abundant cell in skeleton, forming a complex functional network with neighboring osteocytes as well as with cells involved in skeletal adaptation (*e.g.*, bone lining cells, mesenchymal stem cells, osteoclast precursors). Thus, current dogma suggests that osteocytes perceive changes in applied strain and coordinate the activity of cells involved in bone adaptation. What remains incompletely understood are the cellular and molecular mechanisms involved in, and required fo, coordinating an adaptive response.

Rodents and humans lacking the *Sost* gene demonstrate a robust high bone mass phenotype characterized by excessive osteoblast activity, demonstrating that *Sost* functions to inhibit bone formation. We have previously shown that osteoanabolic mechanical loading decreases *Sost* expression in a strain-dependent manner[4] and, using a transgenic approach, that suppression of *Sost* is required for load-induced bone formation[7]. *In vitro* studies have suggested that sclerostin, through antagonizing Lrp5/Lrp6-mediated stabilization of β-catenin, directly decreases osteoprogenitor proliferation or matrix maturation and mineralization by osteoblasts [19]. In contrast, the influence of sclerostin on osteoclasts appears to be indirect, mediated through an autocrine mechanism of sclerostin on osteocytes to regulate RANKL and OPG levels[20]. Functionally, pharmacologic inhibition of sclerostin activity by *in vivo* administration of a neutralizing antibody increases bone mass and strength in animal models of osteoporosis[21–23], enhances fracture repair[24–26], and prevents bone loss under disuse conditions [5,27].

Less attention has been focused on understanding the cellular and molecular mechanisms involved in regulation of endogenous *Sost* transcription. Initial studies by Sutherland *et al.* demonstrated that bone morphogenetic proteins (BMPs) [28] increase *Sost* expression. Subsequent studies found that numerous osteotropic growth factors and hormones—including parathyroid hormone[29], prostaglandin E_2[30], transforming growth factor-beta[13], tumor necrosis factor-alpha[31]—regulate *Sost* expression through either the distal

enhancer or its proximal promoter, suggesting that altering *Sost* transcription is required for these agents to elicit skeletal effects. Deletion of a 52kb element 35kb downstream of the *SOST* gene produces the human autosomal recessive skeletal dysplastic disease van Buchem disease[9], revealing that non-coding elements contribute to *SOST* expression. Using cross-species sequence comparison of the 52kb element deleted in van Buchem disease, we identified an enhancer element, termed *ECR5*, that drives *Sost* expression in *in vitro* and developmentally[11]. Deletion of the ECR5 distal enhancer decreases osteocytic expression of *Sost* to create a high bone mass phenotype[12]. We have found *in vitro* that the effect of certain osteotropic growth factors on *Sost* transcription, such as transforming growth factor-β, is mediated through the ECR5 enhancer rather than the proximal *Sost* promoter[13].

In light of our *in vitro* observation that MEF2 and Smad3 mediate *Sost* expression *via ECR5,* and our *in vivo* results demonstrating that loss of *ECR5* reduces *Sost* expression in osteocytes, we sought to determine whether $ECR5^{-/-}$ mice respond similarly to $Sost^{-/-}$ mice when challenged with a similar anabolic loading stimulus. We found no difference in overall histomorphometric parameters between wildtype and $Sost^{-/-}$ mice across three different strains, demonstrating that the periosteal osteogenic response to loading does not require *Sost*. These findings are consistent with those of Tu *et al.*, wherein reductions in *Sost* expression are permissive for load-induced bone formation[7], but *Sost* expression itself is not *a priori* a fundamental requirement for an osteoanabolic response to load. These results are consistent with our recent report that postnatal b-catenin deletion from Dmp1-expressing osteocytes does not attenuate periosteal load-induced bone formation [32]

Load-induced periosteal bone formation occurs normally (*i.e.*, at wildtype levels) in the absence of *Sost*, though small changes in the distribution of load induced bone formation were noted when Sost was deleted. Wildtype mice demonstrate greater bone formation rates in regions of higher strain (medial and lateral cortices) compared to regions of lower strain (cranial and caudal), whereas rBFR/BS in $Sost^{-/-}$ mice was decreased relative to wildtype mice in high strain regions but increased relative to wildtype mice in low strain regions (Figures 2A–C). We have previously demonstrated that load-induced decreases in sclerostin protein expression is very mild at low strain cranial and caudal regions compared to the more dramatic decrease observed in the high strain medial and lateral cortices [4], suggesting that load-induced bone formation is inversely proportional to sclerostin abundance at a local level. In the absence of *Sost*, however, lower strains at the cranial and caudal cortices are then permissive to initiate bone formation. Thus, a new function for *Sost* in the skeleton is suggested, wherein it serves a s spatial coordinating mechanism that preferentially directs new bone to high strain regions and away from low strain regions.

In vitro, our reporter construct screen suggested that the *ECR5* locus is mechanosensitive, as indicated by the significant decrease in luciferase activity among fluid-sheared cells transfected with *ECR5*-containing plasmids, but not those transfected with the human *SOST* promoter or a heterologous SV40 promoter. Although we did not include a positive control for increasing Luciferase activity, Wadwha *et al.* have previously shown, using a very similar model, that fluid flow rapidly increases Luciferase activity driven by the COX-2 proximal promoter [33]. It was therefore surprising that when we followed up on this result *in vivo*, we found no differences in the periosteal response to loading in $ECR5^{-/-}$ mice compared to

wildtype mice. Further, we did not detect the altered distribution of load-induced bone formation that was observed in loaded *Sost*$^{-/-}$ mice. We do not believe that the parameters chosen for the in vitro examination of hSOST promoter and ECR5 mechanoresponsiveness —such as cell line, presence of FBS in flow media, culture conditions—are responsible for the differences observed *in vitro vs. in vivo*. Indeed, the bulk of studies examining the contribution of promoter and enhancer to *Sost* expression have been performed in UMR106.1 cells [11,13,34], and we do not observe significant differences in Luciferase activity for the plasmids used herein when UMR106.1 cells are cultured in 0.1% *vs.* 10% FBS (DC Genetos, unpublished data). Thus, the difference between *in vitro* and *in vivo* results are more likely due to other factors that could not be replicated *in vitro*.

We next examined whether *ECR5* participates in bone loss due to conditions of disuse. Hindlimb suspension for 24 days reduced proximal tibial bone mineral content (Figure 5B) and decreased diaphyseal bone volume (Figure 5C) and trabecular thickness in wildtype (Figure 5D), but not *Sost*$^{-/-}$, mice similar to previously published reports *in vivo* [8]., Thus, *Sost*$^{-/-}$ mice are resistant to the catabolic effects of skeletal unloading. Similarly, inhibition of neuromuscular transmission *via* Botox, cause disuse-induced bone loss in wildtype but not *Sost*$^{-/-}$ mice (Supplemental Figure 1). Like wildtype mice, *ECR5*$^{-/-}$ mice exposed to unloading conditions lost bone, although there was a modest, statistically significant, attenuation of the magnitude of bone loss in *ECR5*$^{-/-}$ mice compared to wildtype mice, although this likely results from increased trabecular bone volume and thickness in *ECR5*$^{-/-}$ compared to wildtype mice prior to hindlimb suspension. Thus, relative loss of trabecular bone was similar in wildtype and *ECR5*$^{-/-}$ mice. Similarly, *Sost* expression was modestly different in wildtype versus *ECR5*$^{-/-}$ mice under disuse conditions, although the relative change in *Sost* was the same between genotypes.

Our results demonstrate that *ECR5* is not required for osteoanabolic or osteocatabolic responses to altered loading conditions. These results were unexpected as we have found that *ECR5* drives *Sost* expression in osteocytes *in vivo* [12], that the ECR5 locus is mechanosensitive (Figure 3), and because ECR5 mediates responsiveness to TGF-b_1 [13], which is activated under loading and is required for load-induced changes in *Sost* expression [35]. Thus, it appears that a locus independent of *ECR5* mediates skeletal mechanosensitivity. Mechanoregulation of *Sost* may instead occur through its proximal promoter, although we found that the human *SOST* promoter transiently increases under *in vitro* loading conditions (Figure 3B). Alternately, other evolutionarily conserved regions in the van Buchem enhancer region [11] may differentially enhance or repress *Sost* expression in response to daily loads versus the relatively higher loads used in this study. Nonetheless, our results demonstrate that the ECR5 osteocyte enhancer is not required for altered *Sost* expression under dynamic loading conditions.

Supplementary Material

Refer to Web version on PubMed Central for supplementary material.

Acknowledgements

Research reported in this publication was supported by National Institute of Arthritis and Musculoskeletal and Skin Diseases of the National Institutes of Health under award numbers R01AR053237 (AGR) and R01AR064255 (DCG), and by National Institute of Diabetes and Digestive and Kidney Diseases of the National Institutes of Health under award number R01DK075730 (GGL). This work was in part performed under the auspices of the U.S. Department of Energy by Lawrence Livermore National Laboratory under Contract DE- AC52-07NA27344. The content is solely the responsibility of the authors and does not necessarily represent the official views of the National Institutes of Health. The funders had no role in study design, data collection and analysis, decision to publish, or preparation of the manuscript.

REFERENCES

[1]. Uhthoff H, Jaworski Z, Bone loss in response to long-term immobilization, J Bone and Joint Surg-British. 60B (1978) 420–429.

[2]. Jaworski Z, Uhthoff H, Reversibility of nontraumatic disuse osteoporosis during its active phase, Bone. 7 (1986) 431–439. [PubMed: 3801236]

[3]. Lanyon LE, Control of bone architecture by functional load bearing, J Bone Miner Res. 7 Suppl 2 (1992) S369–75. doi:10.1002/jbmr.5650071403. [PubMed: 1485545]

[4]. Robling AG, Niziolek PJ, Baldridge LA, Condon KW, Allen MR, Alam I, et al., Mechanical stimulation of bone in vivo reduces osteocyte expression of Sost/sclerostin, J Biol Chem. 283 (2008) 5866–5875. doi:10.1074/jbc.M705092200. [PubMed: 18089564]

[5]. Spatz JM, Ellman R, Cloutier AM, Louis L, van Vliet M, Suva LJ, et al., Sclerostin antibody inhibits skeletal deterioration due to reduced mechanical loading, J Bone Miner Res. 28 (2013) 865–874. doi:10.1002/jbmr.1807. [PubMed: 23109229]

[6]. Spatz JM, Wein MN, Gooi JH, Qu Y, Garr JL, Liu S, et al., The Wnt-inhibitor Sclerostin is Upregulated by Mechanical Unloading in Osteocytes in-vitro, J Biol Chem. (2015) jbc.M114.628313. doi:10.1074/jbc.M114.628313.

[7]. Tu X, Rhee Y, Condon K, Bivi N, Allen MR, Dwyer D, et al., Sost downregulation and local Wnt signaling are required for the osteogenic response to mechanical loading, Bone. (2011). doi: 10.1016/j.bone.2011.10.025.

[8]. Lin C, Jiang X, Dai Z, Guo X, Weng T, Wang J, et al., Sclerostin mediates bone response to mechanical unloading through antagonizing Wnt/beta-catenin signaling, J Bone Miner Res. 24 (2009) 1651–1661. doi:10.1359/jbmr.090411. [PubMed: 19419300]

[9]. Balemans W, Patel N, Ebeling M, Van Hul E, Wuyts W, Lacza C, et al., Identification of a 52 kb deletion downstream of the SOST gene in patients with van Buchem disease, J Med Genet. 39 (2002) 91–97. [PubMed: 11836356]

[10]. Staehling-Hampton K, Proll S, Paeper BW, Zhao L, Charmley P, Brown A, et al., A 52-kb deletion in the SOST-MEOX1 intergenic region on 17q12-q21 is associated with van Buchem disease in the Dutch population, Am J Med Genet. 110 (2002) 144–152. doi:10.1002/ajmg. 10401. [PubMed: 12116252]

[11]. Loots GG, Kneissel M, Keller H, Baptist M, Chang J, Collette NM, et al., Genomic deletion of a long-range bone enhancer misregulates sclerostin in Van Buchem disease, Genome Research. 15 (2005) 928–935. doi:10.1101/gr.3437105. [PubMed: 15965026]

[12]. Collette NM, Genetos DC, Economides AN, Xie L, Shahnazari M, Yao W, et al., Targeted deletion of Sost distal enhancer increases bone formation and bone mass, Proc Natl Acad Sci USA. 109 (2012) 14092–14097. doi:10.1073/pnas.1207188109. [PubMed: 22886088]

[13]. Loots GG, Keller H, Leupin O, Murugesh D, Collette NM, Genetos DC, TGF-β regulates sclerostin expression via the ECR5 enhancer, Bone. 50 (2012) 663–669. doi:10.1016/j.bone. 2011.11.016. [PubMed: 22155511]

[14]. Li X, Ominsky MS, Niu Q-T, Sun N, Daugherty B, D'Agostin D, et al., Targeted deletion of the sclerostin gene in mice results in increased bone formation and bone strength, J Bone Miner Res. 23 (2008) 860–869. doi:10.1359/jbmr.080216. [PubMed: 18269310]

[15]. Robling AG, Li J, Shultz KL, Beamer WG, Turner CH, Evidence for a skeletal mechanosensitivity gene on mouse chromosome 4, Faseb J. 17 (2003) 324–326. doi:10.1096/fj.02-0393fje. [PubMed: 12490544]

[16]. Jacobs CR, Yellowley CE, Davis BR, Zhou Z, Cimbala JM, Donahue HJ, Differential effect of steady versus oscillating flow on bone cells, J Biomech. 31 (1998) 969–976. [PubMed: 9880053]

[17]. Niziolek PJ, Bullock W, Warman ML, Robling AG, Missense Mutations in LRP5 Associated with High Bone Mass Protect the Mouse Skeleton from Disuse- and Ovariectomy-Induced Osteopenia, PLoS ONE. 10 (2015) e0140775. doi:10.1371/journal.pone.0140775. [PubMed: 26554834]

[18]. Papanicolaou SE, Phipps RJ, Fyhrie DP, Genetos DC, Modulation of sclerostin expression by mechanical loading and bone morphogenetic proteins in osteogenic cells, Biorheology. 46 (2009) 389–399. doi:10.3233/BIR-2009-0550. [PubMed: 19940355]

[19]. ten Dijke P, Krause C, de Gorter DJJ, Löwik CWGM, van Bezooijen RL, Osteocyte-derived sclerostin inhibits bone formation: its role in bone morphogenetic protein and Wnt signaling, J Bone Joint Surg Am. 90 Suppl 1 (2008) 31–35. doi:10.2106/JBJS.G.01183.

[20]. Wijenayaka AR, Kogawa M, Lim HP, Bonewald LF, Findlay DM, Atkins GJ, Sclerostin Stimulates Osteocyte Support of Osteoclast Activity by a RANKL-Dependent Pathway, PLoS ONE. 6 (2011) e25900. doi:10.1371/journal.pone.0025900. [PubMed: 21991382]

[21]. Li X, Ominsky MS, Warmington KS, Morony S, Gong J, Cao J, et al., Sclerostin antibody treatment increases bone formation, bone mass, and bone strength in a rat model of postmenopausal osteoporosis, J Bone Miner Res. 24 (2009) 578–588. doi:10.1359/jbmr.081206. [PubMed: 19049336]

[22]. Ominsky MS, Vlasseros F, Jolette J, Smith SY, Stouch B, Doellgast G, et al., Two doses of sclerostin antibody in cynomolgus monkeys increases bone formation, bone mineral density, and bone strength, J Bone Miner Res. 25 (2010) 948–959. doi:10.1002/jbmr.14. [PubMed: 20200929]

[23]. Zhang D, Hu M, Chu T, Lin L, Wang J, Li X, et al., Sclerostin antibody prevented progressive bone loss in combined ovariectomized and concurrent functional disuse, Bone. 87 (2016) 161–168. doi:10.1016/j.bone.2016.02.005. [PubMed: 26868528]

[24]. Ominsky MS, Li C, Li X, Tan HL, Lee E, Barrero M, et al., Inhibition of sclerostin by monoclonal antibody enhances bone healing and improves bone density and strength of nonfractured bones, J Bone Miner Res. 26 (2011) 1012–1021. doi:10.1002/jbmr.307. [PubMed: 21542004]

[25]. McDonald MM, Morse A, Mikulec K, Peacock L, Yu N, Baldock PA, et al., Inhibition of sclerostin by systemic treatment with sclerostin antibody enhances healing of proximal tibial defects in ovariectomized rats, J Orthop Res. 30 (2012) 1541–1548. doi:10.1002/jor.22109. [PubMed: 22457198]

[26]. Jawad MU, Fritton KE, Ma T, Ren P-G, Goodman SB, Ke HZ, et al., Effects of sclerostin antibody on healing of a non-critical size femoral bone defect, J Orthop Res. 31 (2013) 155–163. doi:10.1002/jor.22186. [PubMed: 22887736]

[27]. Beggs LA, Ye F, Ghosh P, Beck DT, Conover CF, Balaez A, et al., Sclerostin inhibition prevents spinal cord injury-induced cancellous bone loss, J Bone Miner Res. 30 (2015) 681–689. doi:10.1002/jbmr.2396. [PubMed: 25359699]

[28]. Sutherland MK, Geoghegan JC, Yu C, Winkler DG, Latham JA, Unique regulation of SOST, the sclerosteosis gene, by BMPs and steroid hormones in human osteoblasts, Bone. 35 (2004) 448–454. doi:10.1016/j.bone.2004.04.019. [PubMed: 15268896]

[29]. Keller H, Kneissel M, SOST is a target gene for PTH in bone, Bone. 37 (2005) 148–158. doi:10.1016/j.bone.2005.03.018. [PubMed: 15946907]

[30]. Genetos DC, Yellowley CE, Loots GG, Prostaglandin E2 signals through PTGER2 to regulate sclerostin expression, PLoS ONE. 6 (2011) e17772. doi:10.1371/journal.pone.0017772. [PubMed: 21436889]

[31]. Vincent C, Findlay DM, Welldon KJ, Wijenayaka AR, Zheng TS, Haynes DR, et al., ProInflammatory Cytokines TNF-Related Weak Inducer of Apoptosis (TWEAK) and TNFα Induce the Mitogen-Activated Protein Kinase (MAPK)-Dependent Expression of Sclerostin in

Human Osteoblasts*, J Bone Miner Res. 24 (2009) 1434–1449. doi:10.1359/jbmr.090305. [PubMed: 19292615]

[32]. Kang K-S, Hong JM, Robling AG, Postnatal β-catenin deletion from Dmp1-expressing osteocytes/osteoblasts reduces structural adaptation to loading, but not periosteal load-induced bone formation, Bone. (2016). doi:10.1016/j.bone.2016.04.028.

[33]. Wadhwa S, Godwin SL, Peterson DR, Epstein MA, Raisz LG, Pilbeam CC, Fluid flow induction of cyclo-oxygenase 2 gene expression in osteoblasts is dependent on an extracellular signal-regulated kinase signaling pathway, J Bone Miner Res. 17 (2002) 266–274. doi:10.1359/jbmr.2002.17.2.266. [PubMed: 11811557]

[34]. Leupin O, Kramer I, Collette NM, Loots GG, Natt F, Kneissel M, et al., Control of the SOST bone enhancer by PTH using MEF2 transcription factors, J Bone Miner Res. 22 (2007) 1957–1967. doi:10.1359/jbmr.070804. [PubMed: 17696759]

[35]. Nguyen J, Tang SY, Nguyen D, Alliston T, Load regulates bone formation and Sclerostin expression through a TGFβ-dependent mechanism, PLoS ONE. 8 (2013) e53813. doi:10.1371/journal.pone.0053813. [PubMed: 23308287]

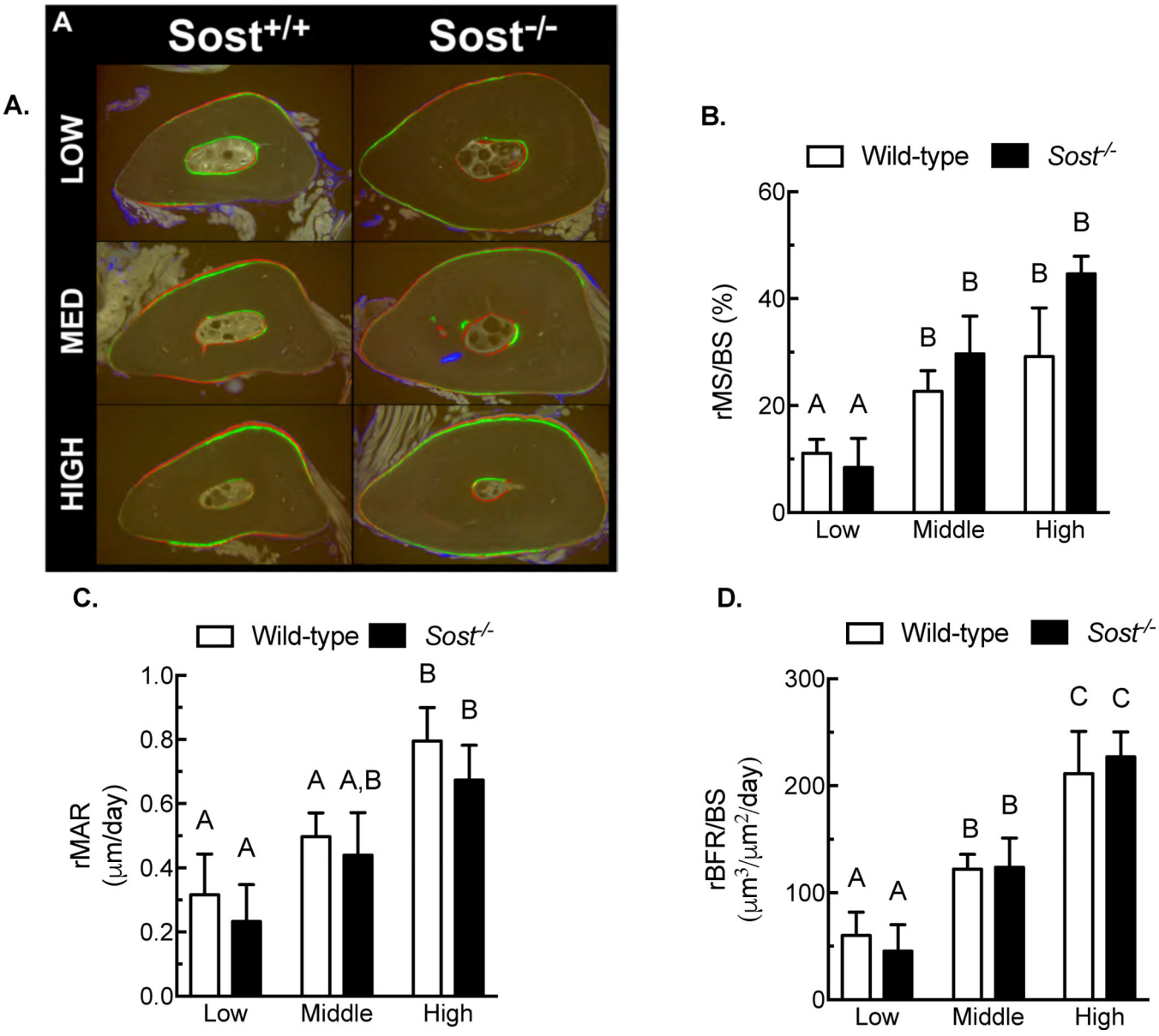

Figure 1. Wild-type and *Sost*$^{-/-}$ mice demonstrate similar periosteal anabolic responses to mechanical loading.

(A) Photomicrographs of fluorochrome-labeled ulnar midshaft sections from *Sost*$^{+/+}$ and *Sost*$^{-/-}$ mice loaded *in vivo* 3 days/week for 2 weeks. Load was applied at low (1800 με), medium (2300 με), or high (2800 με) peak strain. Relative mineralizing surface per unit bone surface (rMS/BS; panel **B**), relative mineral apposition rate (rMAR; panel **C**), and relative bone formation rate (rBFR/BS; panel **D**), measured around the entire periosteal surface, were equally and dose-responsively elevated in wild-type and *Sost*$^{-/-}$ mice as a result of loading. Different letters denote statistical differences among groups. n = 9–10/group.

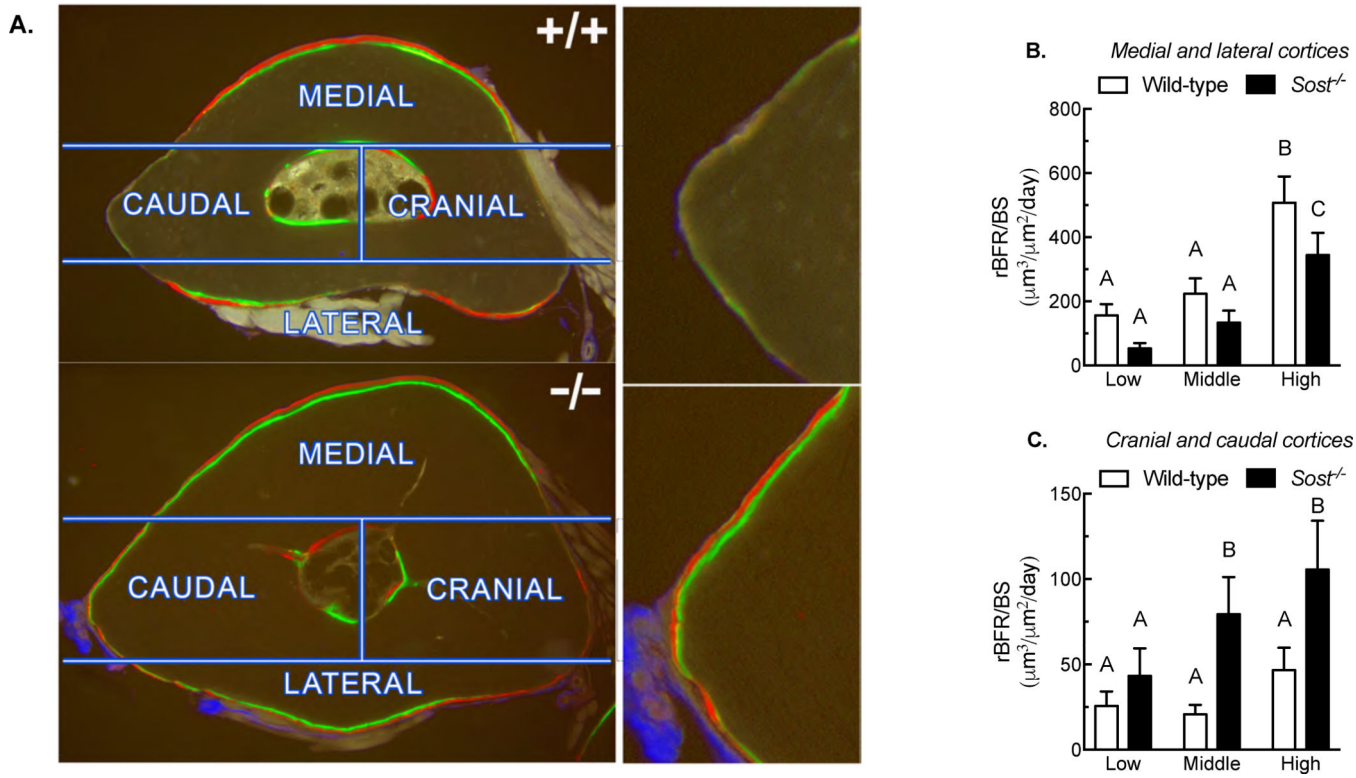

Figure 2. Distribution of new load-induced bone formation to high and low strain regions of the ulnar periosteal surface in wild-type and *Sost*$^{-/-}$ mice.

(**A**) Photomicrographs of fluorochrome-labeled ulnar sections with superimposed sectors used to partition bone formation measurements. The images reveal increased labeling along the neutral axis (caudal and cranial sectors) and decreased bone formation in the high strain sectors (medial and lateral sectors) in *Sost*$^{-/-}$ mice, compared to wild-type mice (*images on right side of panel A are close-up views of the caudal cortex from the left panels*). Quantification of bone formation rates pooled for high strain (medial and lateral) (**B**) and low strain (cranial and caudal) (**C**) regions indicate that *Sost*$^{-/-}$ mice were less efficient at localizing bone to the high strain surfaces than were wild-type mice. Different letters denote statistical differences among groups. n = 9–10/group.

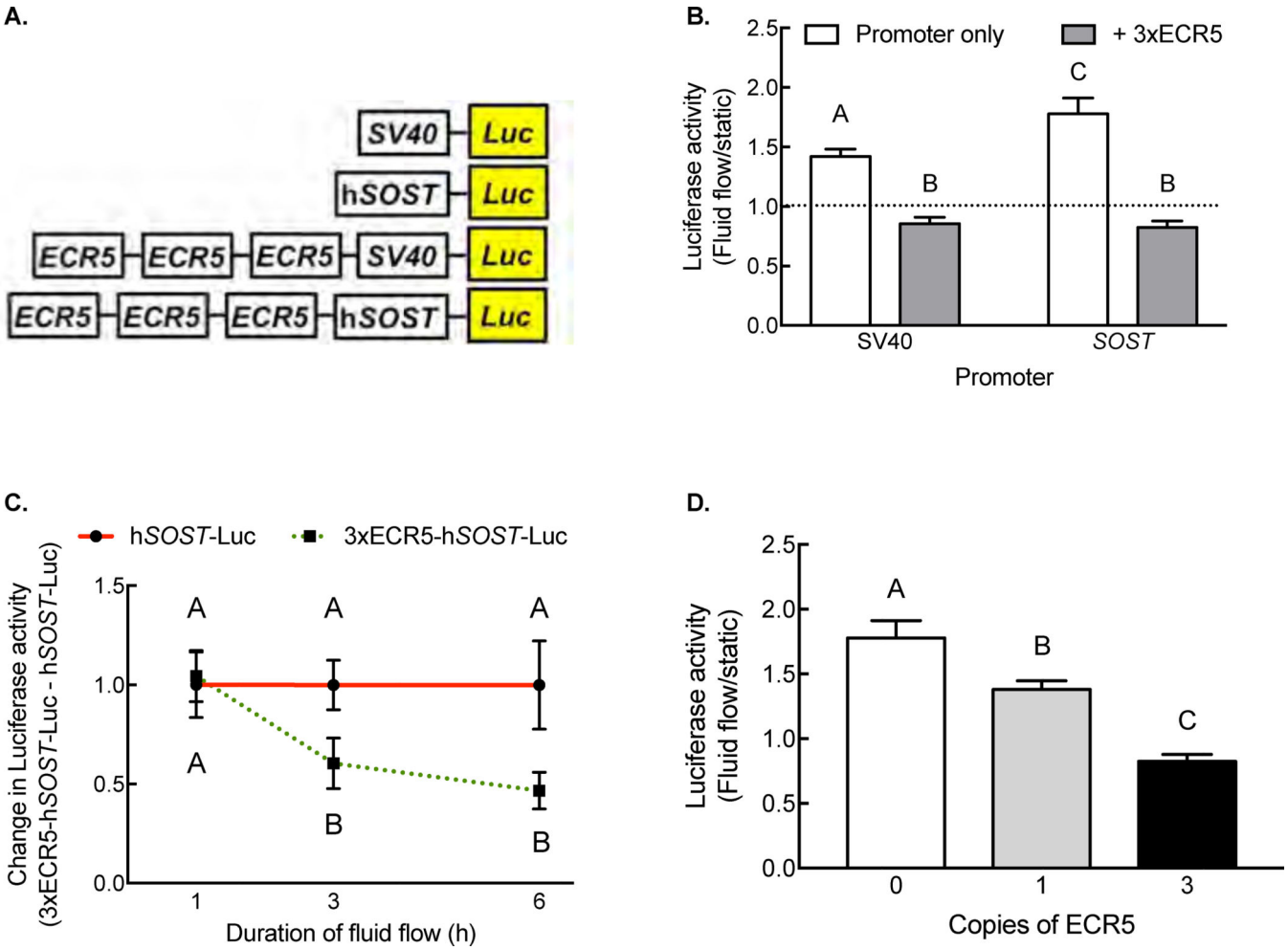

Figure 3. The ECR5 enhancer is mechanosensitive.

(A) Diagram of Luciferase plasmids under control of heterologous SV40 promoter, the 2kb human *SOST* promoter, in the absence of presence of three copies of *ECR5*. **(B)** Oscillatory fluid flow significantly increased Luciferase activity in cells transfected with heterologous SV40 or *SOST* promoter, whereas plasmids containing *ECR5* decreased Luciferase activity in response to fluid flow. **(C)** Time course of suppression of *ECR5*-driven Luciferase activity. **(D)** Dose-dependent effect of *ECR5* copy number on Luciferase activity. Different letters denote statistical differences among groups.

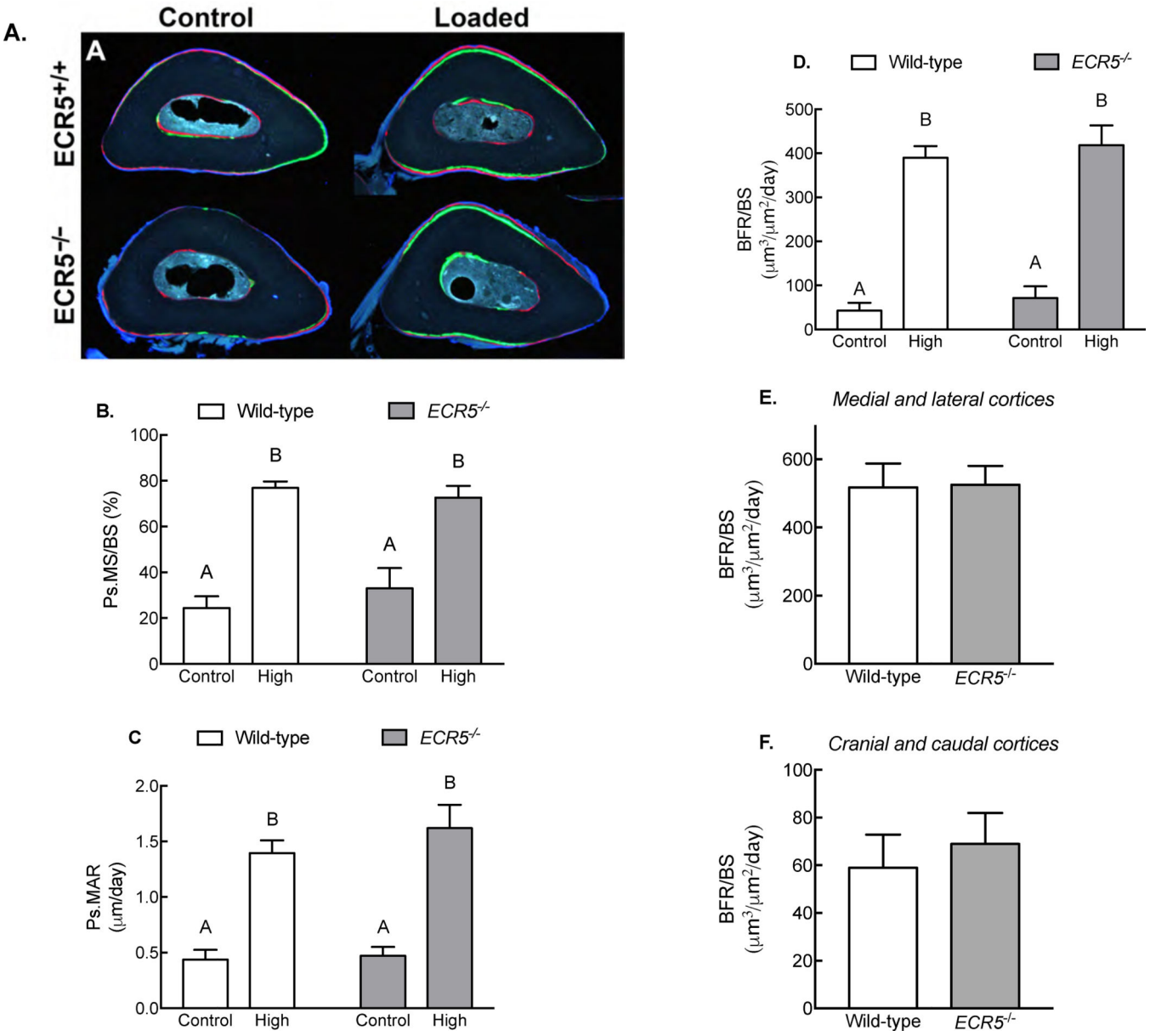

Figure 4. Load-induced bone formation in the absence of ECR5.

(A) Photomicrographs of fluorochrome-labeled ulnar midshaft sections from wild-type and *ECR5*$^{-/-}$ mice loaded *in vivo*, 3 days/week for 2 week. Load was applied at 2800 με peak strain. Relative mineralizing surface per unit bone surface (rMS/BS; panel **B**), relative mineral apposition rate (rMAR; panel **C**), and relative bone formation rate (rBFR/BS; panel **D**), measured around the entire periosteal surface, were equally elevated in wild-type and *ECR5*$^{-/-}$ mice as a result of loading. Quantification of bone formation rates pooled for low strain regions and for high strain regions indicate that wild-type and ECR5$^{-/-}$ mice were equally efficient at localizing new bone to the high strain surfaces. Different letters denote statistical differences among groups. n = 7–9/group.

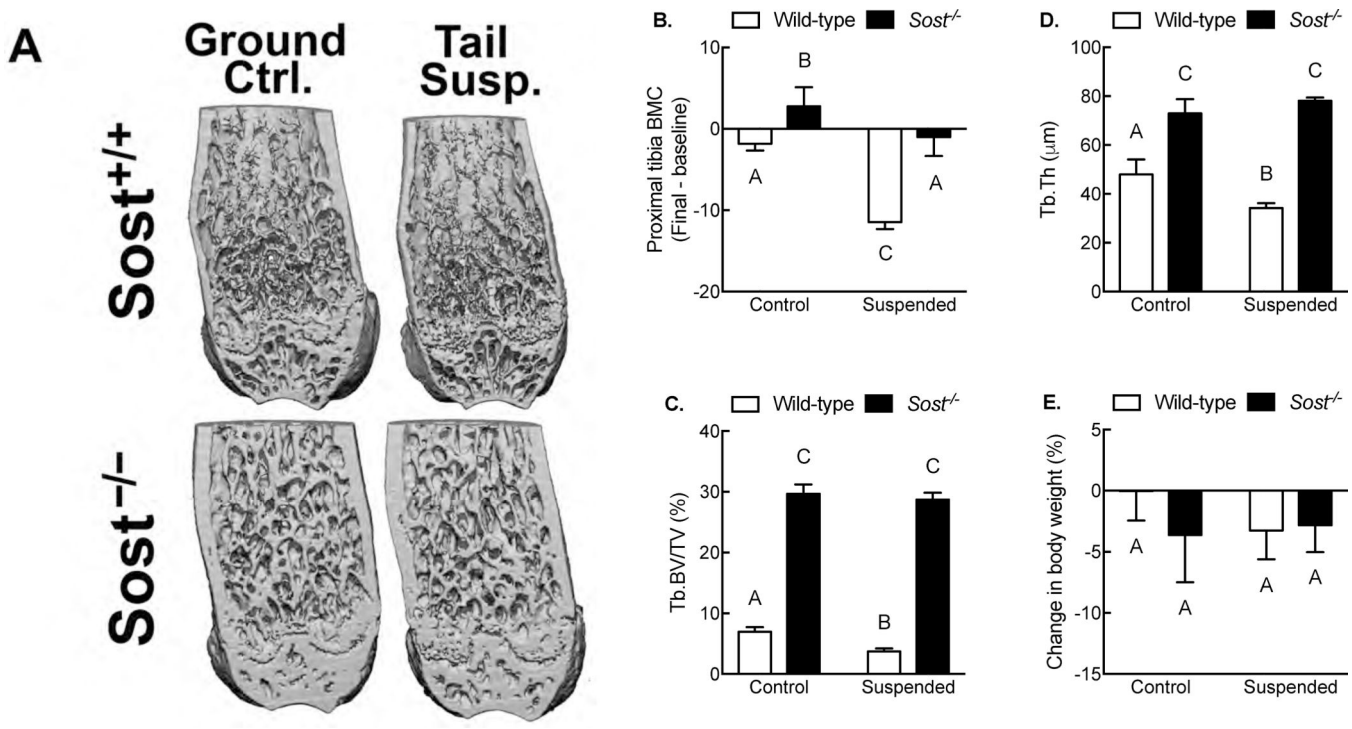

Figure 5. *Sost* is required for bone wasting under disuse conditions.

(A) Representative μCT reconstructions of the distal femur from ground control and tail-suspended wild-type and *Sost*$^{-/-}$ mice. **(B)** Percent change (pre-suspension scan vs. post-suspension scan) in proximal tibia bone mineral content from ground control and tail-suspended wild-type and *Sost*$^{-/-}$ mice as measured by serial pQCT scans. Bone volume fraction (**C**) and trabecular thickness (**D**) in the distal femur metaphysis as measured by μCT. (**E**) Percent change (pre-suspension vs. post-suspension) in body mass in ground control and tail-suspended wild-type and *Sost*$^{-/-}$ mice. *p<0.05 for tail suspended mice vs genotype-matched control mice. Different letters denote statistical differences among groups. n = 8–10/group.

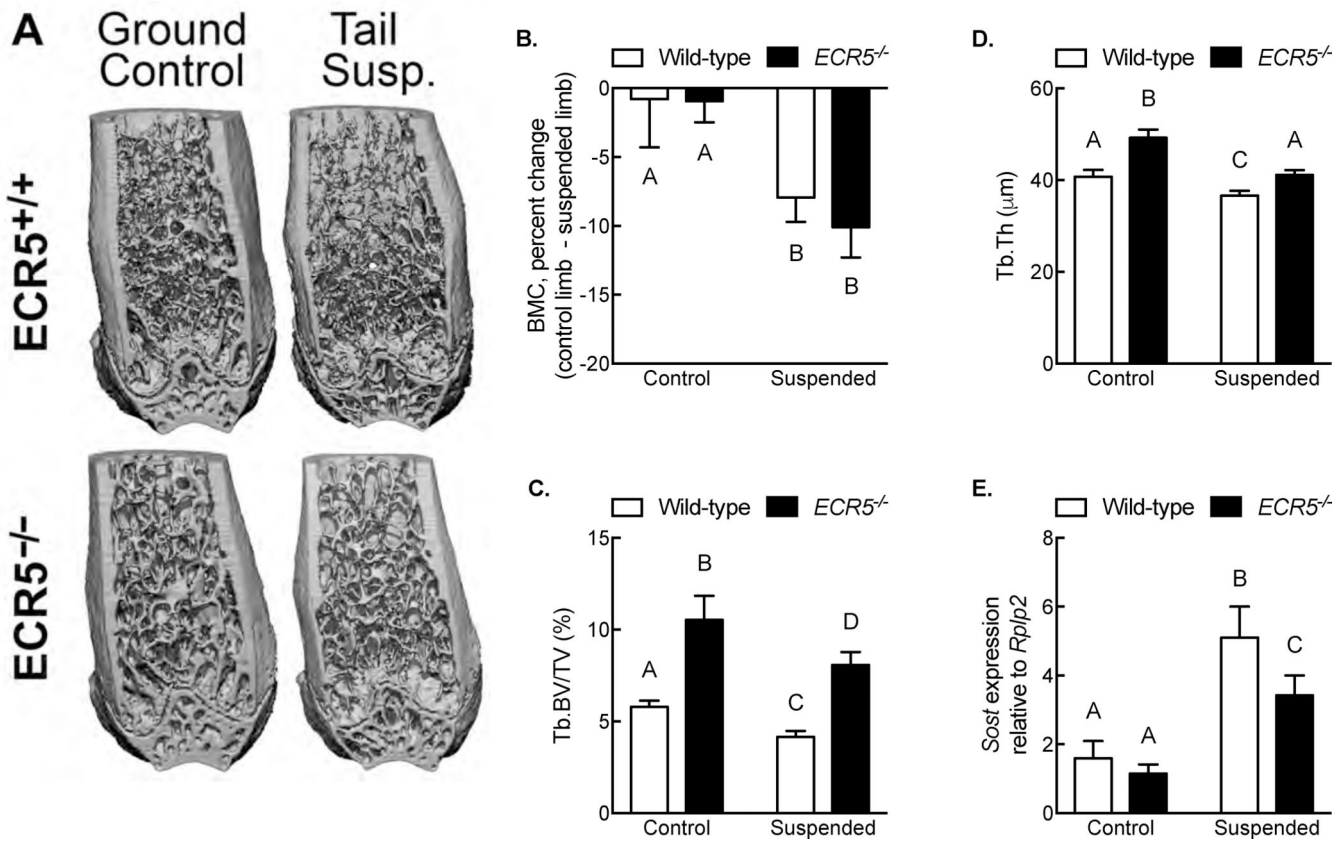

Figure 6. *ECR5* is not required for bone wasting under disuse conditions.

(A) Representative μCT reconstructions of the distal femur from ground control and tail-suspended wild-type and *ECR5*$^{-/-}$ mice. **(B)** Percent change (pre-suspension scan vs. post-suspension scan) in proximal tibia bone mineral content from ground control and tail-suspended wild-type and *ECR5*$^{-/-}$ mice as measured by serial pQCT scans. Bone volume fraction (**C**) and trabecular thickness (**D**) in the distal femur metaphysis as measured by μCT. (**E**) Relative expression of *Sost* transcript, normalized to the housekeeping gene *Rplp2*, in the tibia and femur cortex of ground control and tail-suspended wild-type and *ECR5*$^{-/-}$ mice. Different letters denote statistical differences among groups. n = 8–10/group for panels **B–D**; n = 6/group for panel **E**.